Research article

Journal of RAMAN SPECTROSCOPY

Received: 30 January 2012 Revised: 23 April 2012 Accepted: 11 May 2012 Published online in Wiley Online Library: 16 July 2012

(wileyonlinelibrary.com) DOI 10.1002/jrs.4131

Effect of shape and interstice on surface enhanced Raman scattering (SERS) of molecules adsorbed on gold nanoparticles in the near-dipole and quadrupole regions

T. Abdallah,[a] T.A. El-Brolosy,[a] M. B. Mohamed,[b] K. Easawi,[c] S. Negm[c] and H. Talaat[a]*

Surface enhanced Raman scattering (SERS) of adsorbed molecule on colloidal gold nanoparticles of different shapes, namely nanospheres (NSs), nanorods (NRs), and nanoprisms (NPs) as well as the three NPs arrays of different interstice prepared by NS lithography, are studied with incident wavenumbers in the near-dipole and near-quadrpole regions of the nanoparticles. In the colloidal gold nanoparticles, the SERS enhancement is the largest for the sharp tip followed by the truncated tip NPs, then the NRs and least enhancement for the NSs. This decreasing order of enhancement occurs although the incident wavenumber was near the dipole resonance of NSs and the quadrupole resonance for the NPs. These varied enhancements are explained in part as due to the binding energies of the nanocrystal facets, but the larger contribution results from the plasmon electromagnetic fields. A parallel finite difference time domain (FDTD) calculations were carried out, which corporate the experimental results and show agreement with ratios of the SERS enhancement for the different shapes. The normalized SERS intensity for NPs of different interstice distances show a sharp rise with the decrease of the interstice distances because of interparticle dipolar and quadrupolar coupling as evidenced also by FDTD calculations. Furthermore, these calculations show that the enhancement is polarization independent for an incident wavelength near quadrupole resonance but polarization dependent for an incident wavelength near the plasmon dipole transition. In the last case, the enhancement is larger by an order of magnitude for a polarization parallel to the NPs bisector than for polarization normal to the bisector with no hot spots for the relatively large interstice dimensions used.

Supporting information may be found in the online version of this article.

Keywords: SERS; plasmonics; nanostructures

Introduction

Since the discovery more than 3 decades ago, of surface enhanced Raman scattering (SERS) of molecules adsorbed on specially prepared metal surfaces, the plasmonic nature of the enhancement has been formulated to account for this process. In such an enhancement, the spectra of molecules show intensities that can increase up to 14 orders of magnitudes[1,2] of what is excepted (in the absence of these substrates). This enhancement allows the possibility for single molecule spectroscopy[3–6] which has a great impact in other fields of biology and medicine, in addition to the fundamental spectroscopic studies of the molecules. It is generally accepted that this plasmonic-induced enhancement accounts for up to 12 orders of magnitude[7] and others like chemical effects may account for the other enhancements. These large plasmonic enhancements are caused by the resonant surface plasmons associated strong electromagnetic (EM) fields in the metallic nanostructrures substrates. The extensive observations of SERS of molecules on metal island films (~5 nm)[8] and on silver and gold aqueous colloidal solutions[9] have shown that SERS is truly a nanostructure phenomenon that depends on localized surface plasmon resonances rather than surface effect.[1,10] These localized surface plasmons are coherent oscillations of metal electrons in resonance with incident light at a certain wavenumber.[11] These resonances are functionally dependent on the shape (geometry) and size of the metal nanoparticles.[12] Although there is a wealth of experimental and theoretical studies[13–23] to account for the geometry of these metallic nanoparticles, there are few studies in the literature that are concerned with the comparison of the enhancement because of different shapes. Discrete dipole approximation (DDA) calculations have been used to investigate the EM enhancement induced by optical excitation of localized Surface Plasmon Resonance (SPR) of isolated Ag monomers and dimmers.[24] On the other hand, experimental evaluations of the EM enhancement

* *Correspondence to: H. Talaat, Physics Department, Faculty of Science, Ain Shams University, Abbassia Cairo, Egypt. E-mail: hassantalaat@hotmail.com*

a *Physics Department, Faculty of Science, Ain Shams University, Abbassia, Cairo, Egypt*

b *NILES, Cairo University, Giza, Egypt*

c *Department of Physics and Mathematics, Faculty of Engineering, (Shoubra), Benha University Egypt, Cairo, Egypt*

Journal of RAMAN SPECTROSCOPY

involved in the surface enhanced 'resonance' Raman scattering because of Ag monomers, dimmers, trimmers, and tetramers nanoparticles were reported and compared with the corresponding finite difference time domain (FDTD) calculations.[25] There is still a need for experimental comparison of the enhancement because of different shapes in the 'non-resonance' Raman scattering and in the near dipole and/or quadruple resonance region of the Au nanoparticles.[26] In this 'non-resonance' Raman region, the chemical enhancement in SERS may play a significant role in the enhancement.[27] The recent advances in chemical synthesis[28] as well as in nano-lithography[29] techniques have made it possible to perform such comparison. Colloidal particles of shape homogeneity are appropriate systems for studying the effects of the shape of the metal nanoparticles on the SERS. As nanospherical metal particles are transformed into nanorods (NRs) or triangular nanoprisms (NPs),[30–32] the surface plasmon resonances are strongly affected, typically red-shifting, and even splitting into distinctive dipole and quadrupole plasmon modes.[26] On the other hand, nanosphere (NS) lithography and electron beam lithography[33] can be employed to produce more uniform geometry nanoparticles with controllable size and interstice distances.

In this study, we first demonstrate the effect of the shape of the colloidal gold nanoparticle on surface enhanced 'non-resonance' Raman scattering of cetyltrimethyl ammonium bromide (CTAB) acting as surfactant. Therefore, gold nanoparticle of three different shapes, namely, NSs, NRs, and NPs of sharp and truncated tips have been investigated to determine the best effective nanoparticle shape for SERS. Second, we study the SERS for pyridine molecule adsorbed on three different sizes of NPs in array structures prepared by NS lithography (NSL) at varying interstice spacing. Third, a parallel computational study was carried out to calculate the electric field intensity distributions, using FDTD, to corporate our experimental results of SERS response of different shapes and the variation of SERS with NPs interstice spacing.

Experimental

Preparation of colloidal gold nanoparticles of different shapes

Gold nanoparticles of different shapes have been prepared using the seed mediated growth method[34,35] to prepare metallic nanoparticles of different shapes; NSs, NRs, truncated, and sharp NPs in aqueous solution. The different shape colloidal gold nanoparticles are prepared using CTAB as a capping material. Gold NSs were prepared by reducing gold ions using Sodium borohydride. Gold NRs and NPs were prepared via seed-mediated method as described and developed by El-Sayed *et al.*[36] and Murphy *et al*,[37] but with our little modification in order to obtain sharp prism and truncated prism. In a typical method, CTAB-stabilized gold nanoparticles (seed crystals) were prepared by reduction of 5-ml solution containing 1-mM $HAuCl_4$ and 0.2-M CTAB with 1.2 ml of ice cold aqueous 0.01 M $NaBH_4$, whereas 5 ml of an aqueous growth solution containing 0.2-M CTAB, 70 μl of 4-mM $AgNO_3$, and 1-mM $HAuCl_4.3H_2O$ in a test tube. Addition of the CTAB produced a color change from yellow to brown-yellow suggesting the presence of legend-substituted anions such as CTAB–Au^{III} complex, 50 μl of 0.1-M L-ascorbic acid was added and followed by addition of specific volume of the seed crystals solution, were added to the test tube and left without any disturbance. The color of the solution gradually changed within 30–60 min. The key parameter to obtain different shapes of gold NRs, sharp prism, and truncated prism is the amount of Silver ions added and the pH of the solution. For all the chemically synthesized nanoparticles, a droplet of the solution containing the particles was dispersed on the sample holder for scanning tunneling microscope (STM), OMICRON system. After drying in air, they were studied by operating the system in ultra-high-vacuum, (4×10^{-9} Torr) at room temperature. All samples prepared and used for SERS measurement have the exact same gold ions concentration (1 mM). For the micro-Raman measurements, the droplets was deposited on microscope slide and extra care was taken to have the same volume of the colloid before the evaporation of the solvent and the incident beams of the same cross-section area. SERS was performed using HORIBA JOBN YVON Ramanor HG2S spectrometer equipped with a micro-Raman attachment and Ar^+ laser excitation 514.5 nm.

Nanosphere lithography (NSL)

Three different periodic arrays of gold NPs were prepared using NSL method with spheres of three different diameters[38,31,39] to examine the effect of interstice distances on SERS. Quartz slides were used as the substrate and were cleaned in a piranha solution 3:1 H_2SO_4:30% H_2O_2 at 80 °C for 1.5 h. A 5-μl polystyrene (PS) sphere suspension solution was deposited on the quartz slide, the substrate was slowly immersed in distilled water. A monolayer of PS spheres was formed on the surface of the water. One drop of 2% dodecylsodiumsulfate surfactant was then added to the water and an ordered monolayer of PS spheres was formed. After deposition, the PS spheres were removed by sonication in absolute ethanol. The NSL generated arrayes were also investigated using high resolution scanning electron microscopy JEOL 4000EX, as well as the OMICRON STM system

Measurements

The STM images of colloidal gold nanoparticles of different shapes are shown in Fig. 1 (a–d), the images show that the diameter of gold NSs is ~20 nm, the gold NRs are of length 38 nm and width 20 nm, the truncated and sharp tip gold NPs are of bisector 12 and 14 nm, respectively. The UV-visible absorption spectra for the colloidal prepared samples have been obtained using Ocean Optics USB 2000 spectrometer. The absorption was recorded within the appropriate scan range from 190 to 1100 nm. Fig. 1 (e) shows the absorption spectra for the four shapes of nanoparticles as indicated. The plasmon dipole absorption peak for gold NSs occurs at about 535 nm. The diople and quaderupole modes for NSs are not dintinguishable from one another.[40] It is noticed that this peak has a resemblance in all the shapes used but with much reduced intensity. These reduced peaks in the case of NPs are assigned to the presence of a largely reduced number of the NSs that are formed concomitantly and mixed with higher multipoles of the modulated shape nanoparticles. The rod-shaped gold nanoparticles absorption spectrum shows two absorption bands, the first peak is at 535 nm because of coherent electronic oscillation along the width of the rods (transverse plasmon diople mode). The second absorption band, that appears at 712 nm is caused by the oscillation of the free electrons along the rod axis (the longtudinal plasmon diople mode). This second peak is generally much more intense than the first and has been normally used for SERS and other enhancement of optical phenomena. The relatively larger than excepected intensity of the transverse mode is caused by the same dimensionality of the NRs diameter and the residualy formed NSs diameter. The sharp-tipped gold NPs have their corresponding peaks at 535, 615, and at 705 nm and the truncated tip NPs have their peaks at 535, 593, and 730 nm. The first peak in each spectrum of NPs is assigned as

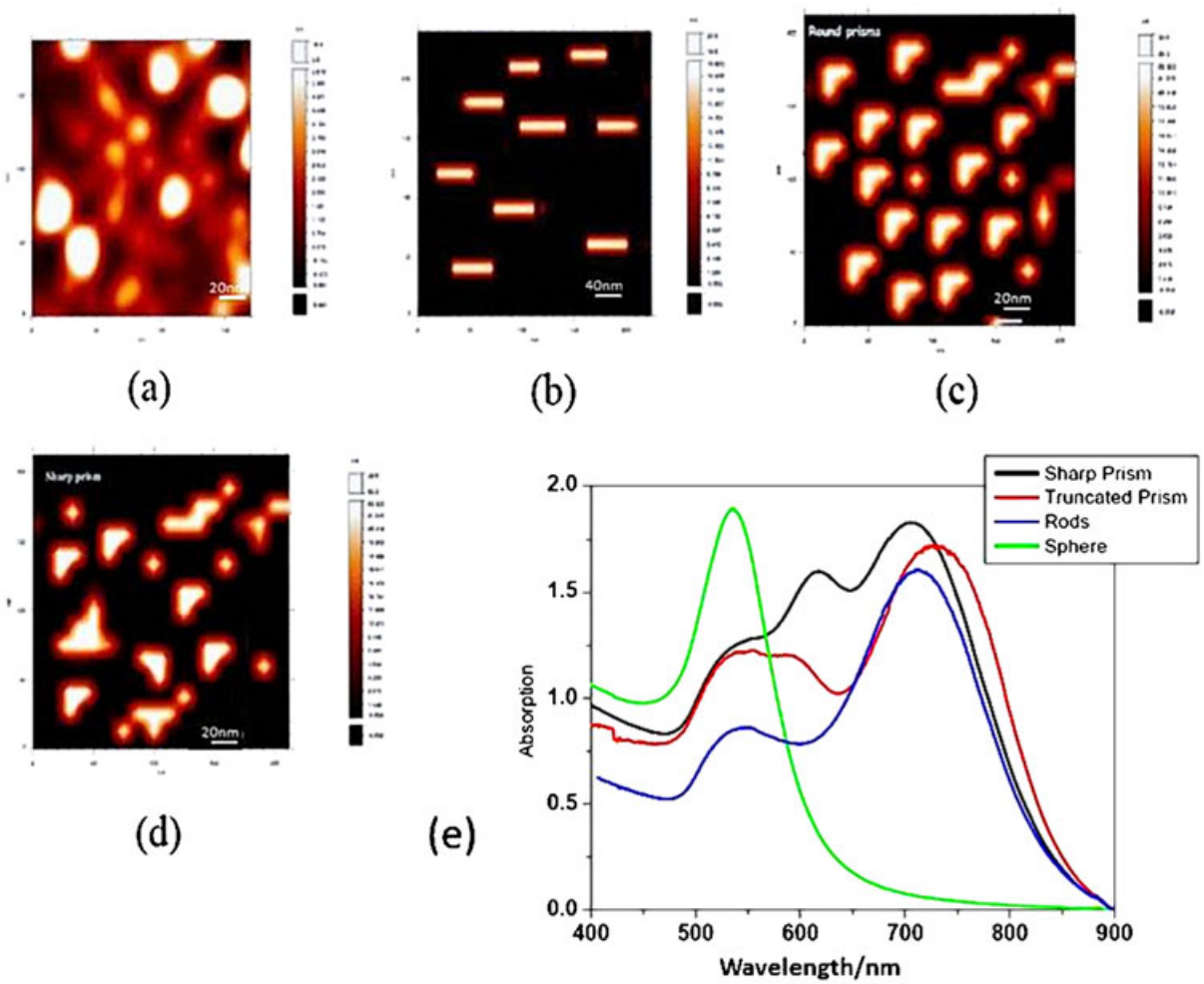

Figure 1. STM images of gold nanoparticles different shapes (a) NSs, (b)NRs, (c) truncated tip NPs, and (d) sharp tip NPs. (e) The optical absorption of collide gold nanopaarticles of different shapes. This figure is available in colour online at wileyonlinelibrary.com/journal/jrs

mentioned before, to the residual NSs mixed with the out of plane quadrpole of NPs, the second peak to the in-plane quadrupole, and the third peak to the in-plane NPs diople.[41] The in-plane dipole plasmon results from the electron cloud moving parallel or antiparallel to the incident field, whereas the quadrupole results from part of the electron cloud moving parallel and the other part moving antiparallel. It is noticed that the in-plane quadrupole peak for the truncated tip NPs is blue shifted, whereas the dipole is red shifted relative to the sharp tip NPs. This is because of the electron cloud density changes across the particle surface.[42] The ability to resolve these modes (quadrupole and dipole) in the case of NPs is a result of their strong anistropicity.

The STM measurements for NSL prepared NPs arrays are presented in Fig. S1(a), which show that the NPs are of bisectors 60, 80, and 100 nm with an interstice (center to center) given by 103, 144, and 200 nm, respectively. Fig. S1(b) shows the high resolution scanning electron microscopy images for the first case, whereas the other images are given in the supporting information Fig. S2.

Results and discussion

Surface enhanced Raman scattering spectra of CTAB acting as surfactant on the colloidal gold nanoparticles are shown in Fig. 2 for the four different shapes used. The SERS were measured at an incident Ar^+ line 514.5 nm that is near to the dipole resonances of the NSs, the transverse modes of NRs, and the out of plane quadrupole of the NPs. The measured spectra are in a good

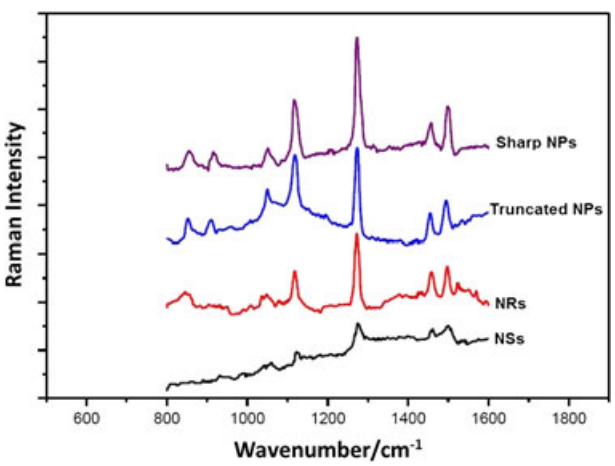

Figure 2. Raman spectra of CTAB as surfactant for collodial gold nanoparticles of different shapes indicated in Fig. (1).

Journal of RAMAN SPECTROSCOPY

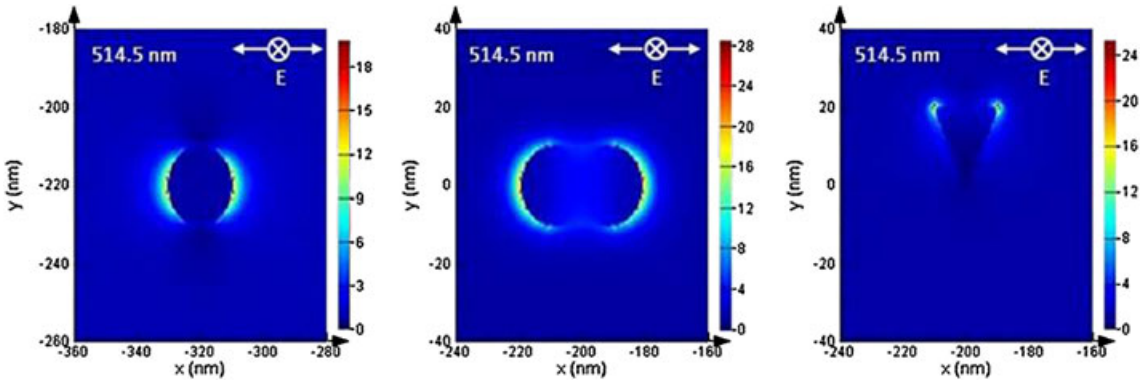

Figure 3. FDTD for field intensity around gold nanoparticles (a) NS, (b) NR, and (c) sharp NP for an incident wavelength 514.5 nm near the dipole of the NS, the transverse dipole for NR, and out of plane quadrupole of NP at the indicated polarization. This figure is available in colour online at wileyonlinelibrary.com/journal/jrs

agreement with the regular Raman spectrum for CTAB.[43] The enhanced peaks are highest for the sharp-tipped NPs, followed by the truncated NPs and NRs. At a clearly less SERS intensity is the spectrum for the NSs in spite of the fact that the incident radiation is near-resonance to the NSs plasmon dipole. The variation in the enhancement may be explained by considering first the chemical reactivity of the different crystal facets at the end of the growth process. Because in these near dipole and near quadruple resonance plasmon coupling of the nanoparticles and non-resonance Raman scattering of CTAB, chemical enhancement becomes an important issue and may be comparable with the EM enhancement. Second, the geometric effects represented by the ratio of surface area to volume (S/V) per unit volume for each shape; NSs, NRs, and NPs, which would eliminate the size effect. Third, the EM enhancement due to plasmonic field distribution of the three shapes, which can be calculated using FDTD.

It is known that CTAB having halide ions would bind to the gold surfaces via the Br^-, with binding energies that scale with [{111} > {110} > {100}].[44] It is also known that the growth direction of the NRs is [100] with the {110} facet along their length, (absent in the case of NSs), which would result in a larger binding of CTAB to the NRs than the NSs, leading to a larger enhancement. In the case of NPs, the {111} crystal facet compose the broad triangular faces of the NPs while they lie at the end of the NRs.[45] Furthermore, I^- (which was proved to be present in commercial CTAB[8]) has great affinity to the {111} facet, that in addition to the strong binding of CTAB to the {112} that composes the sides of the triangular NPs[26] would result in a better enhancement of NPs than NRs. These taken together would partly explain the observed variation of enhancement because of chemical effects with the morphology of the nanoparticles. As for the other channel of the enhancement because of surface area, the S/V ratio per unit volume was calculated for our nanoparticles samples and stands as 6.56, 5.20, and 4.84 for the NPs, NRs, and NSs, respectively. These decreasing ratios, in addition to the aforementioned arguments, may elucidate the observed scaled SERS for the different shape nanoparticles in addition to the surface plasmon EM fields discussed in the following.

The contribution of surface plasmon field enhancement in SERS was estimated using FDTD calculations version 7.5.3.[46] These calculations would determine the field intensity distribution in and around the three nanoparticles shapes, NSs, NRs, and the sharp tip NPs of the same dimensions as those measured by STM. In order to compare with the experimental results, the calculations were carried out for an incident wavelength 514 nm, for two polarizations, one along a particular axis of symmetry and the second normal to it. The computed FDTD results are shown in Fig. 3, where the highest field intensities are 13, 18.2, and 22 for NSs, NRs, and for NPs, respectively. As expected for NSs, there is no change in the field intensity of the two normal polarizations because of symmetry. However, in the case of NRs with the polarization along the length of the rod (longitudinal plasmon), the field intensity (28) is double that for polarization across the diameter (transverse plasmon) (14) (see Fig. 3) (see the supporting information for the other polarization Fig. S3), although the incident wavenumber is closer to the transverse mode resonance. The aforementioned values are almost an order of magnitude smaller than the computed values for silver nanoparticles reported in reference,[24] using discrete dipole approximation. In the case of NPs, the field enhanced intensity is localized at the tips of the prisms that is parallel to the polarization direction. Accordingly, the ratio of the increase in the SERS effective field (E^4) for the NPs to that of the NSs is 2.42, whereas for NRs to NSs is 1.77. These FDTD results are in a reasonable agreement with our experimental observation which gives these ratios as 2.86 for the sharp NPs to NSs and 1.96 for the ratios of NRs to NSs. The fact that the experimental values are larger than the calculated ones is because of the presence of the binding energies of the different shapes facets as discussed earlier. It is to be noticed that the calculations using FDTD version 7.5.3 for the field intensity distribution is a sum over all the multipoles and does not differentiate the contribution for each multipole separately.

The gold NPs fabricated by NSL technique of bisectors 60, 80, and 100 nm with an interstice (center to center) given by 103, 144, and 200 nm, respectively, were employed to investigate the effect of the interstice separation on the SERS enhancement. In this case, we applied pyridine molecules on the NPs structures, so we can study only the effect of interstice distances on the enhancement separate from the role played by chemical activity of the surface facets. The SERS spectra of pyridine molecules adsorbed on the gold NPs with the three different interstice separation as indicated, together with the Raman spectrum of bulk pyridine are shown in Fig. 4. The pyridine wavenumber at 749 and 651 cm^{-1} were used to measure the SERS intensities which show decrease with increasing the separation. To eliminate the size effect of the NPs, we divided the interstice distance **d** by half the bisector **a** of the prisms and plotted ln I_{SERS}

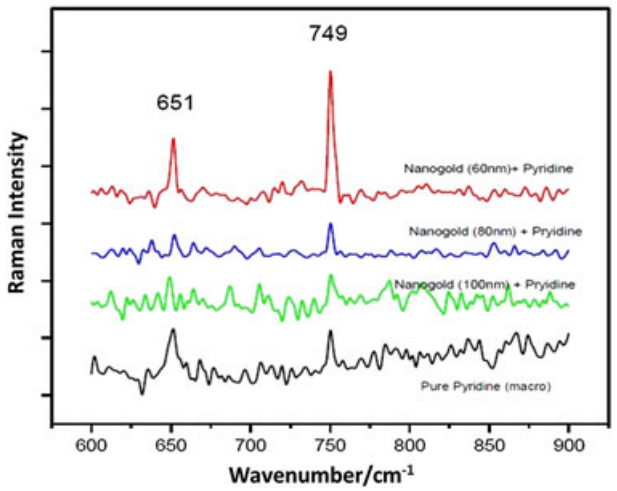

Figure 4. The Raman spectrum of pyridine adsorbed on NPs of different bisectors 60, 80, and 100 nm as indicated.

against **d/a** (Fig. 6 solid lines). The plots show an accelerated decrease in intensity with separation that is characteristic of the interaparticle multimodal coupling that is responsible for the enhancement.[47] The corresponding calculations by FDTD at an incident wavelength 514 nm, near the NPs out of plane quadrupole resonance, and polarization along the bisector (to simulate the experimental results), together with polarization normal to the bisector are shown in the left panel of Fig. 5. The field intensity is localized at the NPs tips parallel to the polarization in each case. These fields are mainly a result of the add mixture of the dipolar and quadrupolar modes with less effect of the former. The localization of the maximum enhancement on the prism tips is also in agreement with the calculations in reference,[24] where they found the maximum enhancement either close to or on the particle, for separation larger than 6 nm. The resulting variations of SERS intensity with interstice separation are shown in Fig. 6 (dash line). In the graph, the FDTD calculated values of field intensities are shown, not on the same scale to indicate the behavior. To examine the enhancement for an incident wavelength close to the dipolar resonance transition for NPs,[48] calculations were also carried out at 673 nm for both polarizations and are shown in the right panel of Fig. 5. In this case, the fields are fully localized at the tips of the NPs parallel to the polarization direction. The field intensity for polarization along the line of apex (along the bisectors) is an order of magnitude larger than for polarization normal to the line of apex. The resulting enhancement in the SERS intensity (E^4) is of order 10^5. Therefore, to exploit the large plasmon dipole field enhancement for head to head NPs dimmers, the incident wavelength should have a polarization along the prisms bisectors in agreement with the discrete dipole approximation in reference.[24] Furthermore, at the relatively large interstice separation used in this work, the computed FDTD enhancement indicate the absence of hot spots in between the NP's and shows as seen in Fig. 6 that the maximum field intensity occurs at the upper tip of the head to head dimmers.

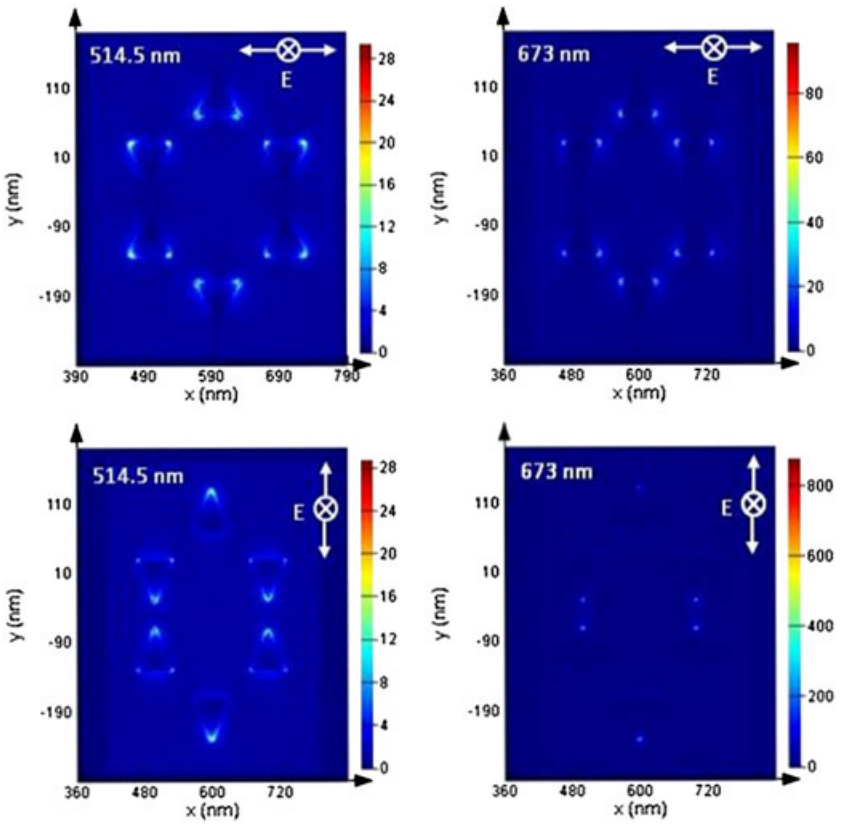

Figure 5. FDTD calculations for the field intensity around gold NPs arrays for particle (a) prism bisector $a = 60$ nm and interstice $d = 103$ nm, (b) prism bisector $a = 80$ nm and interstice $d = 144$ nm, (c) prism bisector $a = 100$ nm and interstice $d = 200$ nm. (d) The SERS intensity for pyridine adsorbed on NPs versus gap/bisector; solid line for Raman lines (left scale), whereas dash line is for In FDTD calculated field intensities (right scale). This figure is available in colour online at wileyonlinelibrary.com/journal/jrs

Journal of RAMAN SPECTROSCOPY

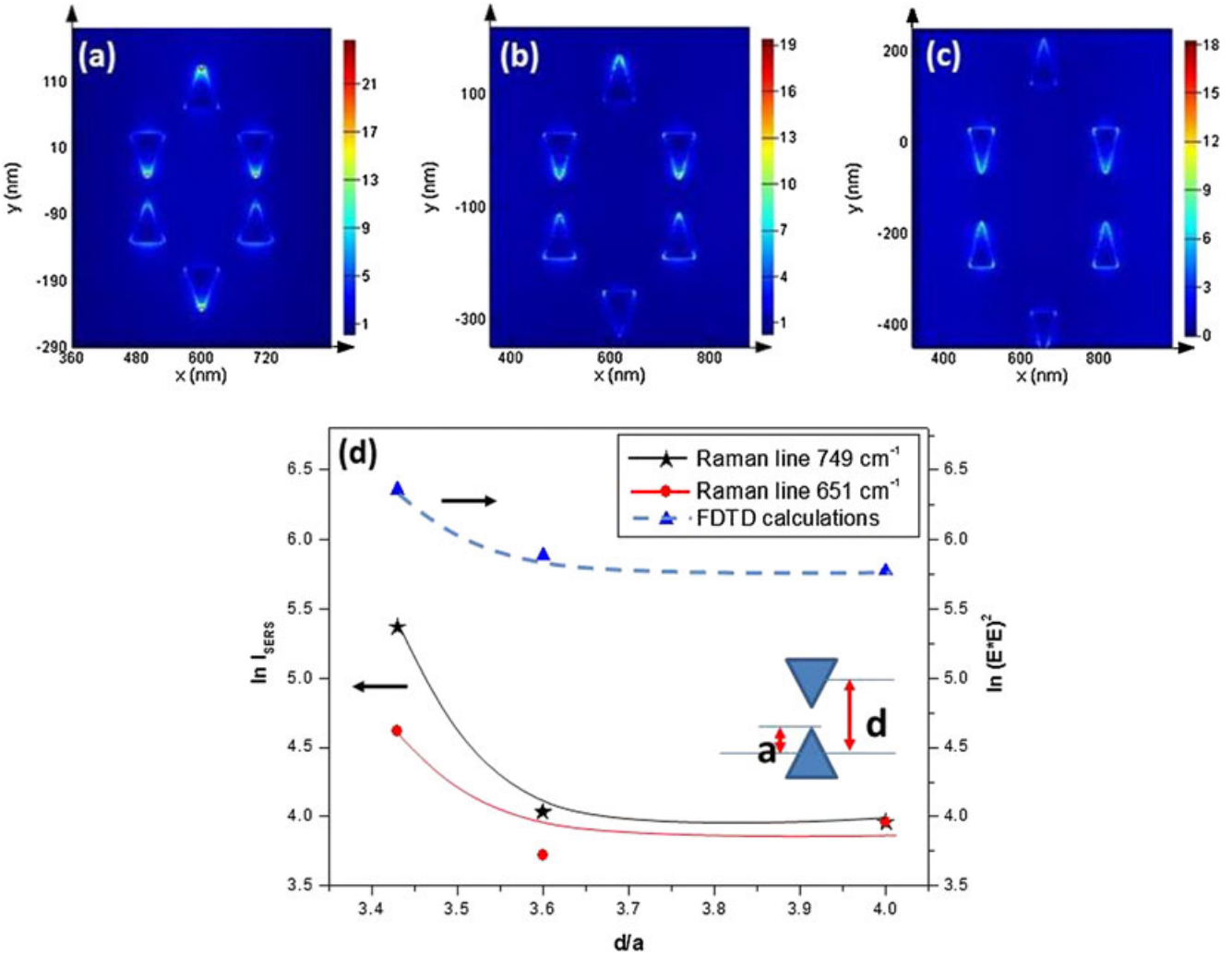

Figure 6. FDTD calculations for the field intensity around gold NPs arrays for particle prism bisector $a = 60$ nm. This figure is available in colour online at wileyonlinelibrary.com/journal/jrs

Conclusions

The SERS of CTAB molecules acting as surfactant adsorbed on NSs, NRs, sharp NPs, and truncated NPs show that the largest enhancement occurs for the sharp tip NPs, followed by the truncated NPs, NRs, and NSs in spite of using an incident wavelength near the dipole resonance of NSs. These enhancements result from being near to the particles quadrupole resonances. The experimentally determined enhancement is larger than the FDTD calculated enhancement because of the additional chemical activity of the facets. The SERS for pyridine adsorbed on NPs at different interstice separation produced by NSL show accelerated decrease as the interstice distances increase, that is, the characteristic of interaparticle multipole coupling. The FDTD calculations for the different configurations give values in reasonable agreement with experimental results. The calculations also indicate that the largest SERS enhancement occurs at the tips of the prisms for the relatively large interstice gaps used with the absence of hot spots.

Acknowledgement

The generous support of the Egyptian STDF grant ID 635 is greatly appreciated. H. T. thanked Prof. M. A. El-Sayed Julius Brown Chair and Regents Professor, School of Chemistry and Biochemistry, Georgia Institute of Technology, Atlanta Georgia USA, for providing the NSL and for the helpful discussions.

Supporting information

Supporting information may be found in the online version of this article.

References

[1] S. J. Lee, Z. Guan, H. Xu, M. Moskovits, *J. Phys. Chem. C* **2007**, *111*, 17985.
[2] Special Issue on SERS, *J. Raman Spectrosc.*, **2005**, *36*(6/7): 465.
[3] K. Kneip, H. Kneip, R. Manoharan, I. Itzkam, R. R. Dasari, M. S. Feld, *Bioimaging.* **1998**, *6*, 104.
[4] P. Johansson, H. Xu, M. Käll, *Phys. Rev. B.* **2005**, *72*, 035427.
[5] H. Xu, X. H. Wang, M. P. Persson, H. Q. Xu, M. Käll, P. Johansson, *Phys. Rev. Lett.* **2004**, *93*, 243002.
[6] H. Xu, E. J. Bjerneld, M. Käll, L. Borjesson, *Phys. Rev. Lett.* **1999**, *83*, 4357.
[7] Nie, S. Emory, S. R., *Science* **1997**, *275*, 1102.
[8] C. Y. Chen, E. Burstein, *Phys. Rev. Lett.* **1980**, *45*, 1287.
[9] C. J. Orendorff, L. Gearheart, N. Jana, C. Murphy, *Phys. Chem. Chem. Phys.* **2006**, *8*, 165.
[10] Z. Q. Tian, B. Ren, J. F. Li, Z. L. Yang, *Chem. Commun.* **2007**, *34*, 3514.
[11] K. A. Willets, R. P. Van Duyne, *Annu. Rev. Phys. Chem.* **2007**, *58*, 267.
[12] K.-S. Lee, M. A. El-Sayed, *Phys. Chem. B.* **2006**, *110*, 19220.

[13] Z. Q. Tian, B. Ren, D. Y. Wu, *J. Phys. Chem. B* **2002**, *106*, 9463.
[14] Z. Q. Tian, B. Ren, *Annu. Rev. Phys. Chem.* **2004**, *55*, 197.
[15] Z. Q. Tian, Z. L. Yang, B. Ren, J. F. Li, Y. Zhang, X. F. Lin, J. W. Hu, D. Y. Wu, *Faraday Discuss.* **2006**, *132*, 159.
[16] Z. Q. Tian, Z. L. Yang, B. Ren, D. Y. Wu, *Top. Appl. Phys.* **2006**, *103*, 125.
[17] Z. Q. Tian, B. Ren, in *Encyclopedia of Electrochemistry*, (Ed.: P. Unwin, A. J. Bard, M. Stratmann, Wiley-VCH, Weinheim, **2003**, *3*, 572.
[18] M. Inoue, K. Ohtaka, *J. Phys. Soc. Jpn.* **1983**, *52*, 3853.
[19] E. C. Le Ru, P. G. Etchegoin, *Chem. Phys. Lett.* **2006**, *423*, 63.
[20] E. Le Ru, J. Grand, N. Félidj, J. Aubard, G. Lévi, A. Hohenau, J. Krenn, E. Blackie, P. Etchegoin, *J. Phys. Chem. C* **2008**, *112*, 8117.
[21] K. Imura, H. Okamoto, M. Hossain, M. Kitajima, *Nano Lett.* **2006**, *6*, 2173.
[22] H. Tamaru, H. Kuwata, H. Miyazaki, K. Miyano, *Appl. Phys. Lett.* **2002**, *80*, 1826.
[23] H. Kuwata, H. Tamaru, K. Esumi, K. Miyano, *Appl. Phys. Lett.* **2003**, *83*, 4625.
[24] E. Hao, G. C. Schatz, *J. Chem. Phys.* **2004**, *120*, 357.
[25] K.-i. Yoshida, T. Itoh, H. Tamaru, V. Biju, M. Ishikawa, Y. Ozaki, *Phys. Rev B.* **2010**, *81*, 115406.
[26] Northwestern University 'PhD Thesis' Millstone, Jill Erin http://gradworks.umi.com/33/31/3331139.html
[27] D.-Y. Wu, J.-F. Li, B. Ren, Z.-Q. Tian, *Chem. Soc. Rev.* **2008**, *37*, 1025.
[28] Y. Sun, Y. Xia, *Science* **2002**, *298*, 2176.
[29] D. Parikh, B. Craver, H. N. Nounu, F.-O. Fong, J. C. Wolfe, *J. Microelectromech. S.* **2008**, *17*, 3.
[30] B. Nikoobakht, M. A. El-Sayed, *Chem. Mater.* **2003**, *15*, 1957.
[31] X. D. Wang, C. J. Summers, Z. L. Wang, *Nano Lett.* **2004**, *4*, 423.
[32] A. W. Kosiorek, P. Kandulski, K. Kempa, M. Giersig, *Nano Lett.* **2004**, *4*, 1359.
[33] R. Negishi, T. Hasegawa, K. Terabe, M. Aono, T. Ebihara, H. Tanaka, T. Ogawa, *Appl. Phys. Lett.* **2006**, *88*, 223111.
[34] J. E. Millstone, W. Wei, M. R. Jones, H. Yoo, C.A Mirkin, *Nano Lett.* **2008**, *8*, 2526.
[35] J. E. Millstone, S Park, K L. Shuford, L Qin, G C. Schatz, C A. Mirkin, *J. Am. Chem. Soc.* **2005**, *127*, 5312.
[36] S. Link, M. B. Mohamed, M. A. El-Sayed, *J. Phys. Chem. B* **1999**, *103*, 3073.
[37] N. R. Jana, G. Latha, C J. Murphy, *Langmuir* **2001**, *17*, 6782.
[38] J. C. Hulteen, R. P. Van Duyne, *J. Vac. Sci. Technol. A* **1995**, *13*, 1553.
[39] W. K Kosiorek, P. Chudzinski, K. Kempa, M. Giersig, *Nano Lett.* **2004**, *4*, 1359.
[40] P. Mulvaney, *Langmuir* **1996**, *12*, 788.
[41] C. Xue, Z. Li, C. A. Mirkin, *Small*, **2005**, *1*, 513.
[42] K. L. Kelly, E. Coronado, L. L. Zhao, G. C. Schatz, *J. Phys. Chem. B* **2003**, *107*, 668.
[43] B. Nikoobakht, J Wang, M A El-Sayed, *Chem. Phys. Lett.* **2002**, *366*, 17.
[44] O. M. Magnussen, *Chem. Rev.* **2002**, *102*, 679.
[45] J. E. Millstone, G. S. Metraux, C. A. Mirkin, *Adv. Funct. Mater.* **2006**, *16*, 1209b.
[46] The simulations were performed by the FDTD Solutions trademark software. http//:www.lumerical.com
[47] E. C. Dreaden, R D. Near, T Abdallah, M. H Talaat, M A. El-Sayed, *Appl. Phys. Lett.* **2011**, *98*, 183115.
[48] W. Huang, W Dian, M A. El. Sayed, *J. Phys. Chem. B.* **2005**, *109*(40): 18881.